Department of Energy, Mines, Industry Regulation and Safety
GOVERNMENT OF WESTERN AUSTRALIA

Geological Survey of Western Australia

Novel geochronology

Can't see for Miles: In situ mica Rb–Sr geochronology from the Rudall Province

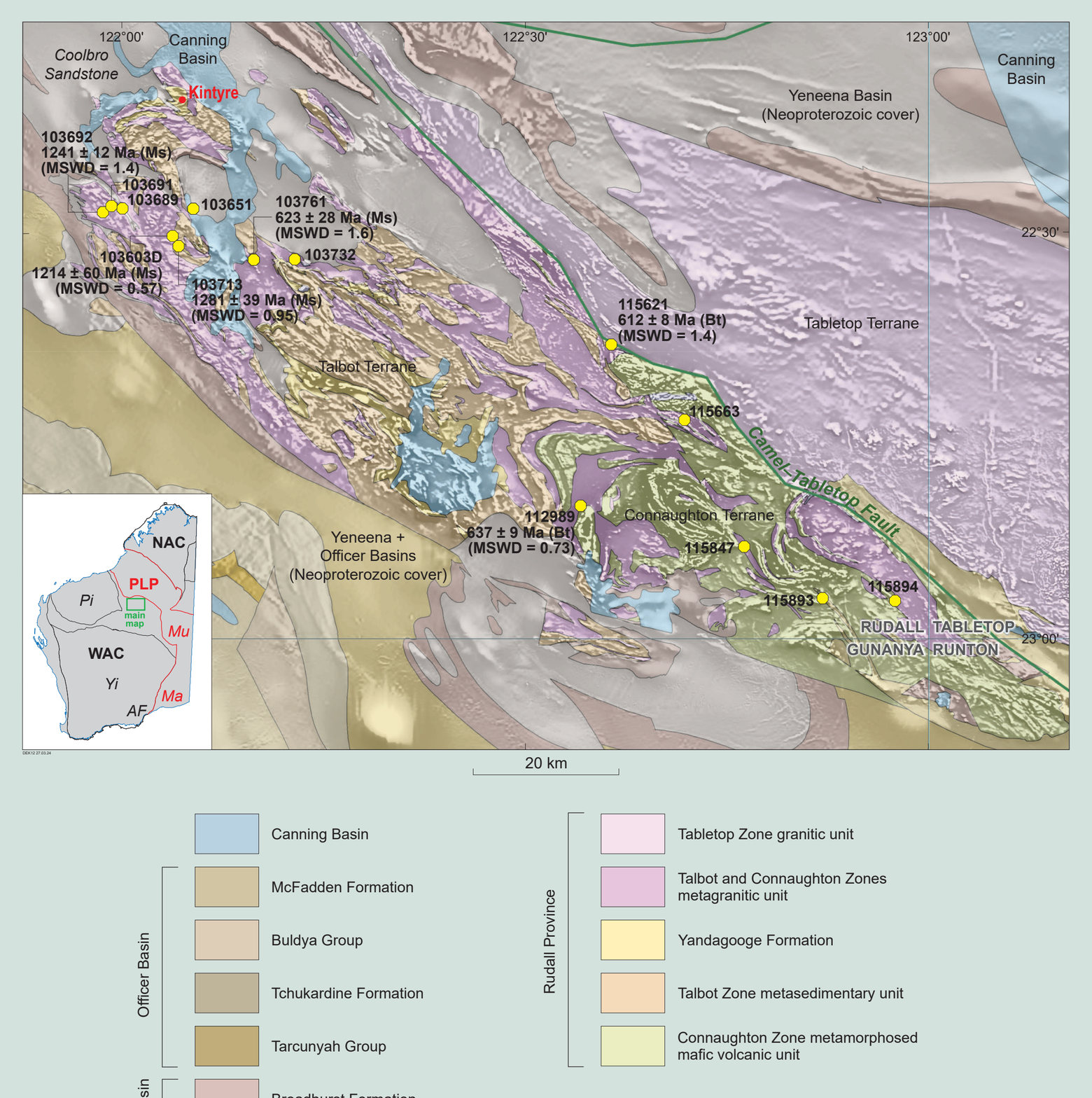

Location map of the Rudall Province, showing the three terranes and the analysed sample locations and isochron dates. Samples with no date label did not define an isochron but rather a spread in data. Coloured geology polygons are taken from the State interpreted bedrock geology polygons 1:500 000 (2016) GIS layer

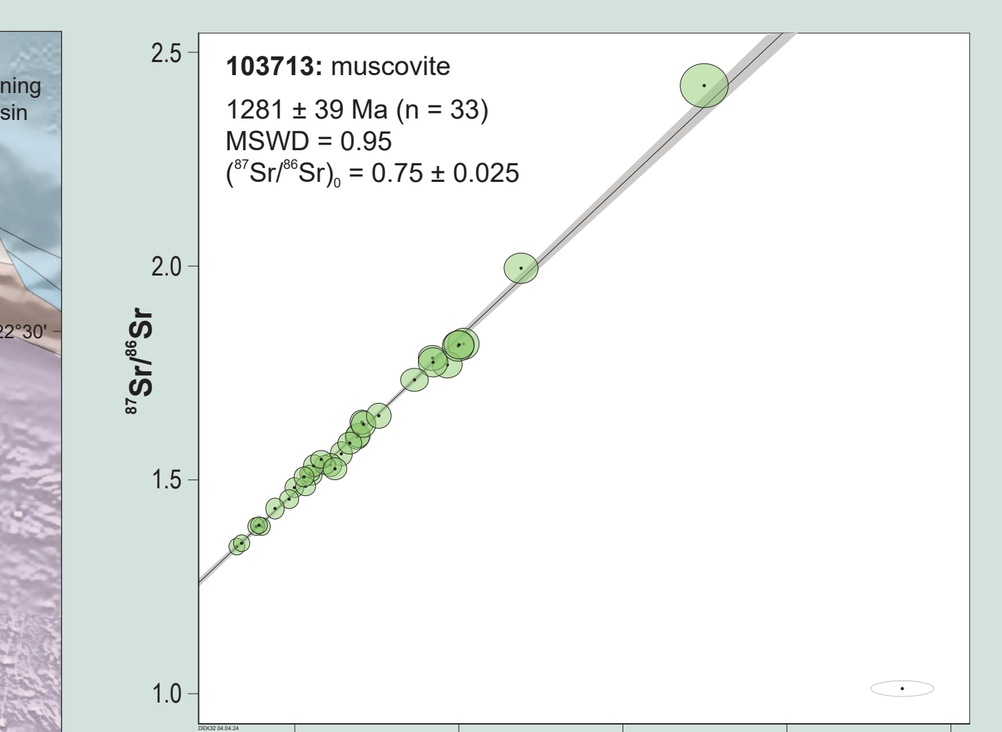

Muscovite Rb–Sr isochron defining a date corresponding to the 1377–1275 Ma Parnngurr Orogeny

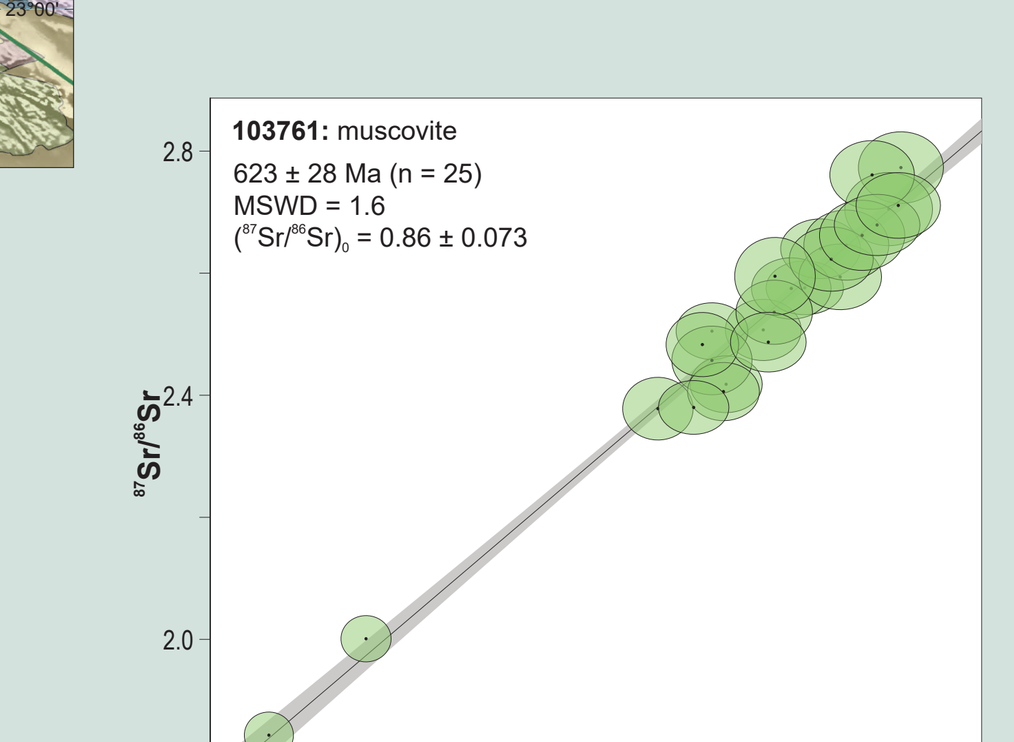

Muscovite Rb–Sr isochron defining a date corresponding to the 654–509 Ma Paterson Orogeny

A longstanding point of conjecture in the evolution of the Paterson Orogen in northern Western Australia is the age of the Neoproterozoic Miles Orogeny. The Miles Orogeny is thought to be characterised in outcrop by regional D3 and D4 structures that were subsequently overprinted by D5 and D6 structures during the 654–509 Ma Paterson Orogeny. However, existing quantitative age constraints for the Miles Orogeny have large uncertainties and define a time frame of approximately 840–750 Ma, all from low-temperature hydrothermal rocks at Nifty mine and Kintyre prospect.

We obtained in situ mica Rb–Sr geochronology from crystalline meta-igneous and metasedimentary rocks within the Rudall Province to try to constrain the age (and existence) of the Miles Orogeny.

Isochrons yielded three Paterson Orogeny ages (623 ± 28 Ma muscovite, 637 ± 9 Ma biotite and 612 ± 8 Ma biotite) and one Parnngurr Orogeny age (1281 ± 40 Ma muscovite). The other two isochrons were 1214 ± 60 Ma (muscovite) and 1242 ± 12 Ma (muscovite). Strikingly, no isochron ages, nor definitive Rb–Sr model ages, were obtained for the Miles Orogeny. Therefore, it is likely that existing and new age data for the proposed Miles Orogeny represent either a hydrothermal fluid flow event, in which case 'Orogeny' is not appropriate terminology, or that it represents mixing of Paterson Orogeny and Mesoproterozoic age components.

Data and Software Centre

Download Report 250 from the DEMIRS eBookshop

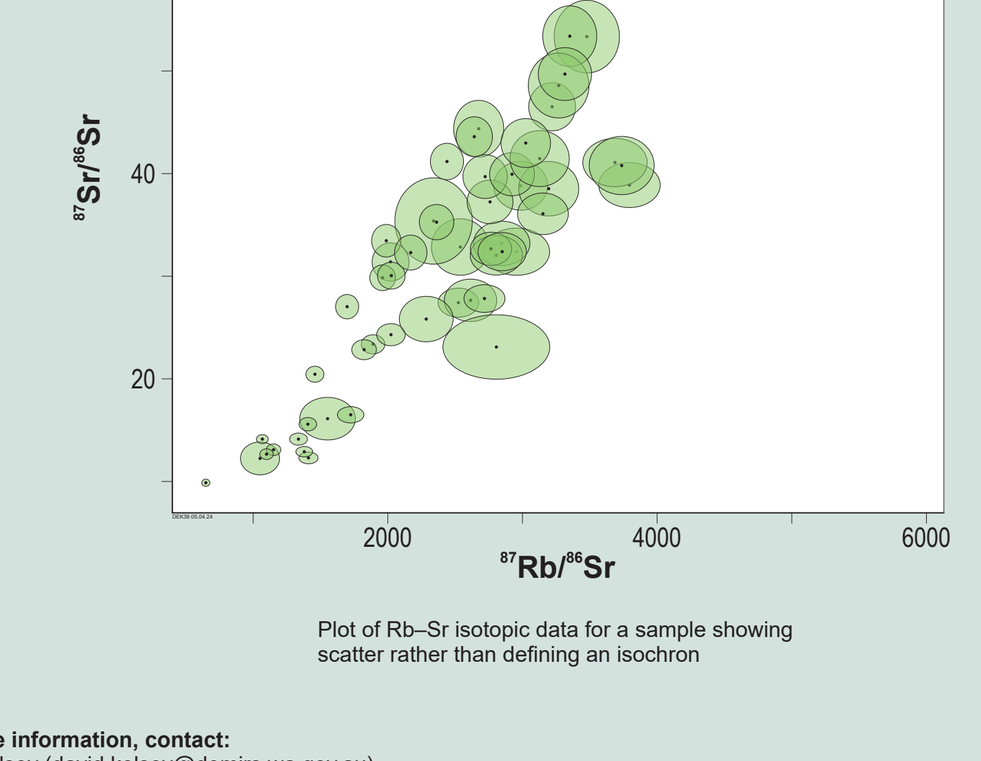

Plot of Rb–Sr isotopic data for a sample showing scatter rather than defining an isochron

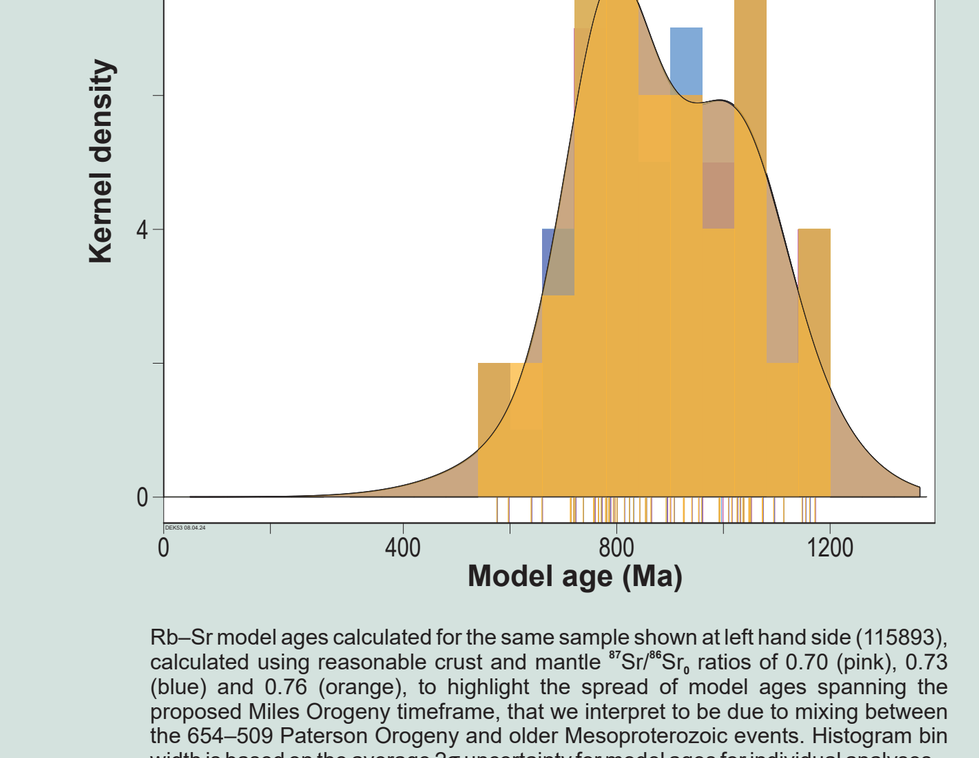

Rb–Sr model ages calculated for the same sample shown at left hand side (115893), calculated using reasonable crust and mantle $^{87}Sr/^{86}Sr_i$ ratios of 0.70 (pink), 0.73 (blue) and 0.76 (orange), to highlight the spread of model ages spanning the proposed Miles Orogeny timeframe, that we interpret to be due to mixing between the 654–509 Paterson Orogeny and older Mesoproterozoic events. Histogram bin width is based on the average 2σ uncertainty for model ages for individual analyses

For more information, contact:
David Kelsey (david.kelsey@demirs.wa.gov.au)

Acknowledgement of Country
The Department of Energy, Mines, Industry Regulation and Safety (DEMIRS) respectfully acknowledges Aboriginal peoples as being the traditional custodians of Western Australia. We acknowledge the enduring connection Aboriginal people continue to share with the land, sea and sky through both their ancestral ties and custodianship to Country. We pay our respect to Elders both past and present, and acknowledge the value brought to our department through the collective contribution of Aboriginal and Torres Strait Islander peoples across Western Australia.

An Archean lithium pegmatite model

GSWA's Archean granite project has acquired a strong Li-bias with sampling now concentrating on the younger low-Ca leucogranite components of both the Yilgarn and Pilbara Cratons. In addition to providing a useful geochemical dataset to Industry, one of our aims is to reconcile field data with prevailing Li-pegmatite models.

Lithium-pegmatites are thought to form either through direct anatexis of Li-rich crust or through extreme fractionation of granitic melts. Geochronological and isotopic data (Kendall-Langley et al., 2020; Lithos, 352–353) strongly favour the latter model for Li-pegmatites in the Archean of Western Australia.

Phanerozoic studies have strongly influenced Li-exploration models which, in the case of granite fractionation models, posit that Li-pegmatite are extracted from granites formed through melting sedimentary-rock dominated crustal source (i.e. S-type granites). Such models are applied to Archean terranes — but the Yilgarn and Pilbara Cratons, which contribute most of the world's hard-rock Li, contain no sedimentary sequences that represent a viable melt source.

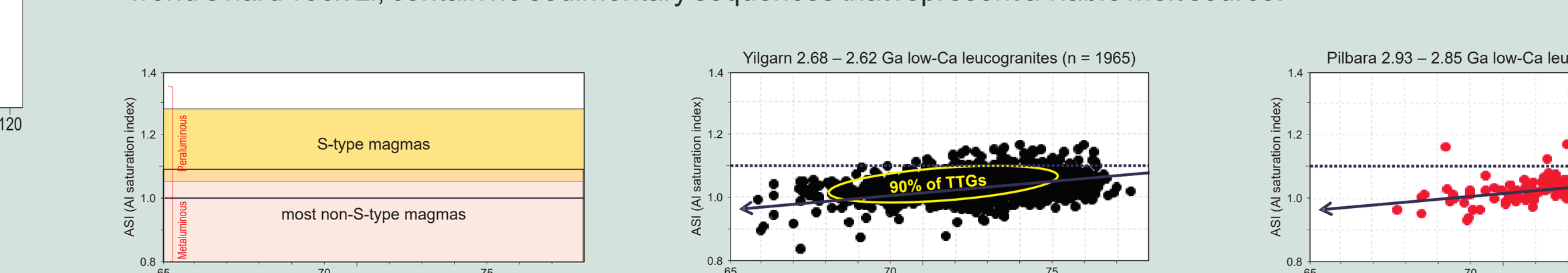

One line of evidence for an absence of melt sources dominated by sedimentary rocks is the complete lack of S-type granites in both cratons. The late, low-Ca leucogranites, which in both cratons are most directly spatially, temporally and compositionally linked with Li-pegmatites, have metaluminous [Aluminium saturation index (ASI) < 1], rather than peraluminous (ASI > 1), parental magmas, precluding a sediment rich source.

The Li-carrying capacity of any crustal melt source is linked to its mica content. With than in mind we look at leucogranite compositions in an attempt to identify mica-rich crustal components, other than metasediments, that might form a crustal melt source.

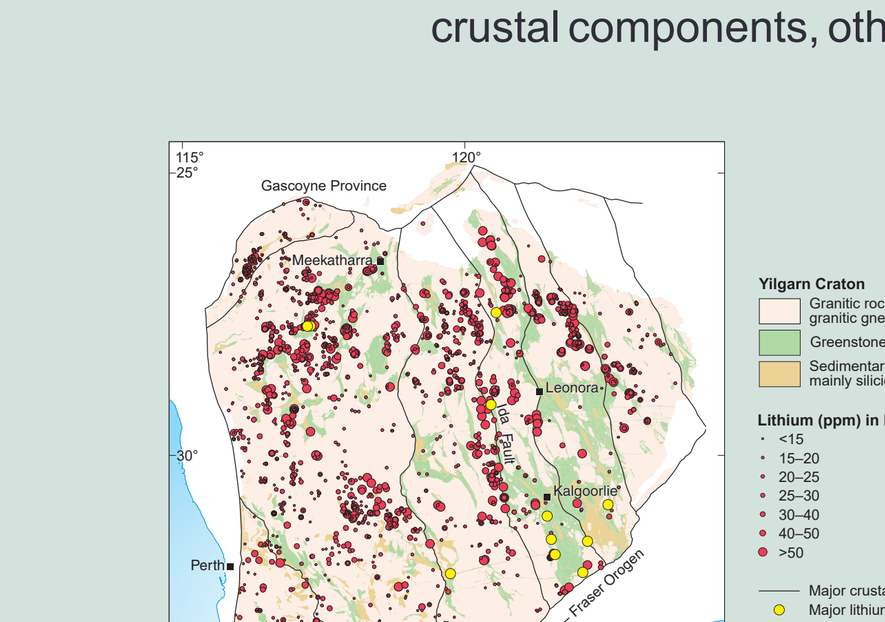

Li-pegmatites in both the Yilgarn and Pilbara Cratons lie along or near contacts between regional granitic crust and greenstone belts (a relationship frequently noted but not understood). Low-Ca leucogranites mainly occupy the granite 'seas' between greenstones belts but become more Li-rich closer to greenstone contacts

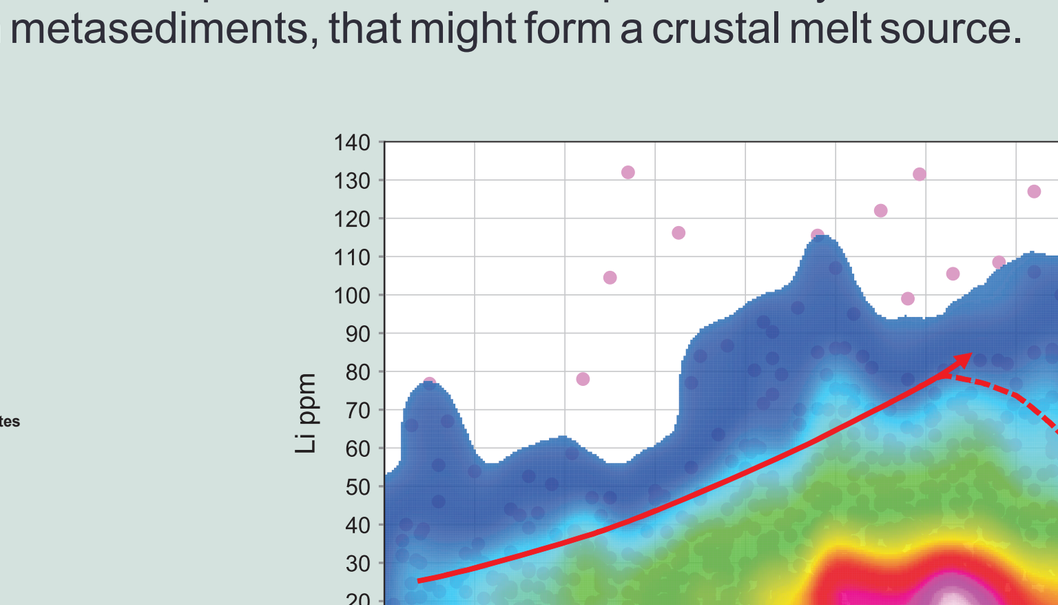

Heat map over Li vs SiO_2 data cloud for low-Ca leucogranites from the Yilgarn Craton. The trend to increasing Li with increasing SiO_2 is the expected igneous trend but the trend to low Li at SiO_2 values above 73–74 wt% most likely reflects primary or secondary loss of Li to the crystallising assemblage. Irrespective, whole rock Li concentrations are a very poor reflection of (minimum) magmatic Li concentrations. Nevertheless, low-Ca leucogranites in the Yilgarn Craton (insufficient data for Pilbara leucogranites) clearly fractionate to 'anomalously' enriched (>30-40 ppm) compositions by ~73 wt% SiO_2

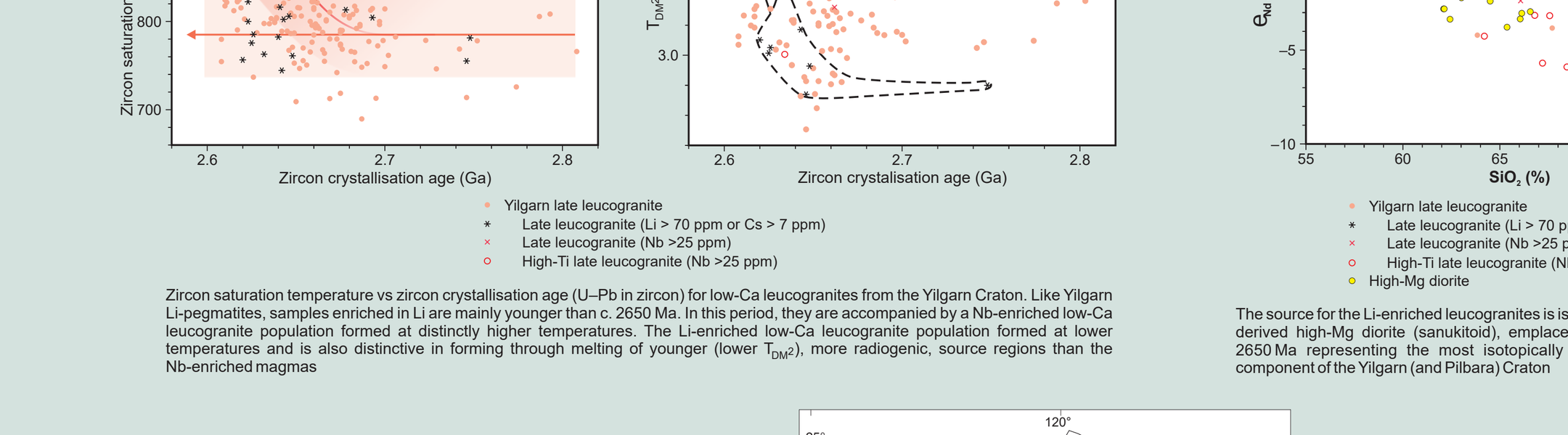

Zircon saturation temperature vs zircon crystallisation age (U–Pb in zircon) for low-Ca leucogranites from the Yilgarn Craton. Like Yilgarn Li-pegmatites, samples enriched in Li are mainly younger than c. 2650 Ma. In this period, they are accompanied by a Nb-enriched low-Ca leucogranite population formed at distinctly higher temperatures. The Li-enriched low-Ca leucogranite population formed at lower temperatures and is also distinctive in forming through melting of younger (lower T_{DM^2}), more radiogenic, source regions than the Nb-enriched magmas

The source for the Li-enriched leucogranites is isotopically similar to that of mantle-derived high-Mg diorite (sanukitoid), emplaced into greenstone belts prior to 2650 Ma representing the most isotopically and chemically primitive felsic component of the Yilgarn (and Pilbara) Craton

These Li-enriched low-Ca leucogranites also concentrate along greenstone–granite contacts, where they contribute to a radiogenic isotopic halo characterising the source of late leucogranites surrounding the greenstone belts. Bottom-of-hole drilling results demonstrate the same relationship (see Pegmatite-hosted lithium prospectivty poster). This supports a connection with Li-pegmatites but intriguingly also indicates that the crustal source region for Li-rich leucogranites was biotite-rich crust adjacent to greenstone belts and comprised fusible material as young and as isotopically juvenile as the high-Mg diorites

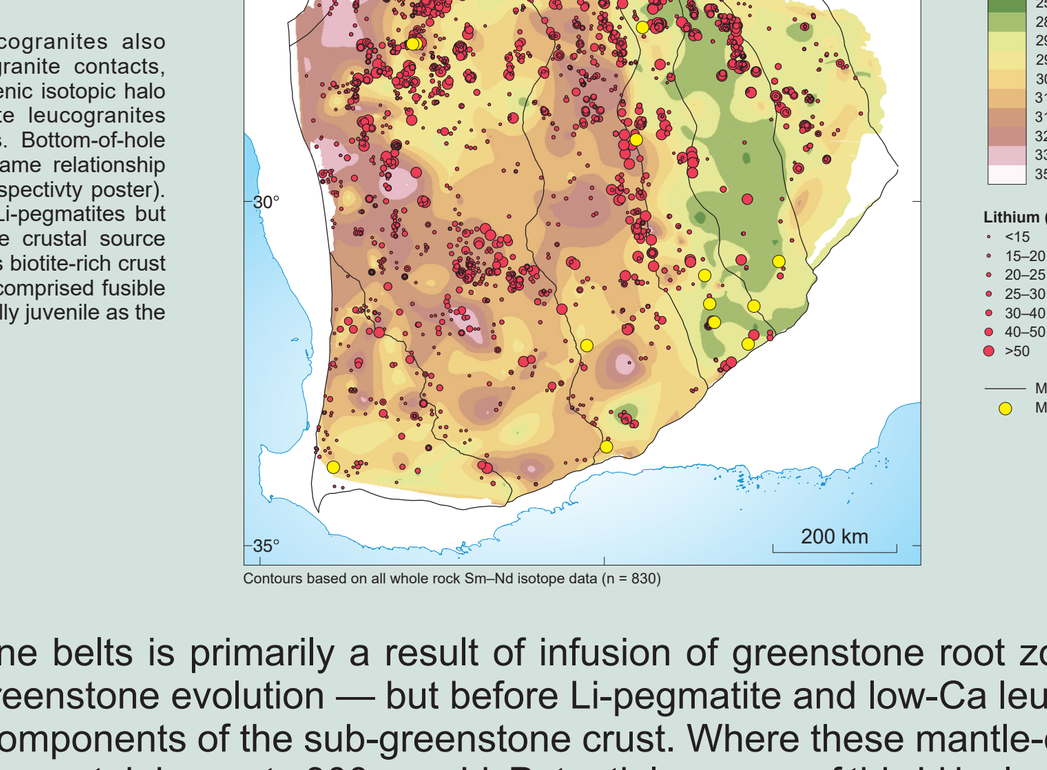

Contours based on all whole rock Sm–Nd isotope data (n = 830)

For more information, contact:
Hugh Smithies (hugh.smithies@demirs.wa.gov.au)

The radiogenic halo surrounding greenstone belts is primarily a result of infusion of greenstone root zones and adjacent crust by strongly hydrated mantle-derived magmas late in greenstone evolution — but before Li-pegmatite and low-Ca leucogranite formation. This hybridised crust reflects one of the most voluminous components of the sub-greenstone crust. Where these mantle-derived intrusions are exposed, they form biotite-rich country rock alteration zones containing up to 300 ppm Li. Potential sources of this Li include sanukitoid-related magmatic fluids (i.e. derived from enriched lithospheric mantle) and Li sequestered from country rock, including seawater altered greenstone.

If no viable 'traditional' source exists for the leucogranites and associated Li-pegmatites in the Yilgarn or Pilbara Cratons, we must look at alternative sources. We are currently investigating the possibility that the required biotite-altered crustal source formed as juvenile, mantle-derived, dioritic magmas (sanukitoid) invaded the root zones of greenstone belts late in greenstone evolution. Melting of this source to produce low-Ca leucogranite, and subsequent fractionation to form pegmatite, explains the empirical spatial link between Li-pegmatite and greenstone–granite contacts as well as the unusually juvenile isotopic signature of Li-enriched Yilgarn leucogranites.

Mineral Systems Atlas

Pegmatite-hosted lithium prospectivity (in prep)

A mineral system-based hybrid *data-rich, knowledge-driven* approach was used to produce a series of predictor maps thought to represent critical components of pegmatite-hosted lithium mineralisation. Predictor maps were calibrated using a dataset of 138 310 exploration drillholes with harmonised maximum lithium grades. Fuzzy logic was employed to combine predictor maps into a final prospectivity map. The results of this map correlate well with known Li resources in Western Australia, and highlight areas for further exploration, while considerably reducing the search area of the State.

Harmonised exploration drillhole data:
a) rank order plot of maximum lithium grade, showing the cut-off grade of 100 ppm used to classify holes as mineralised;
b) distribution of the mineralised (red) and unmineralised (blue) drillholes

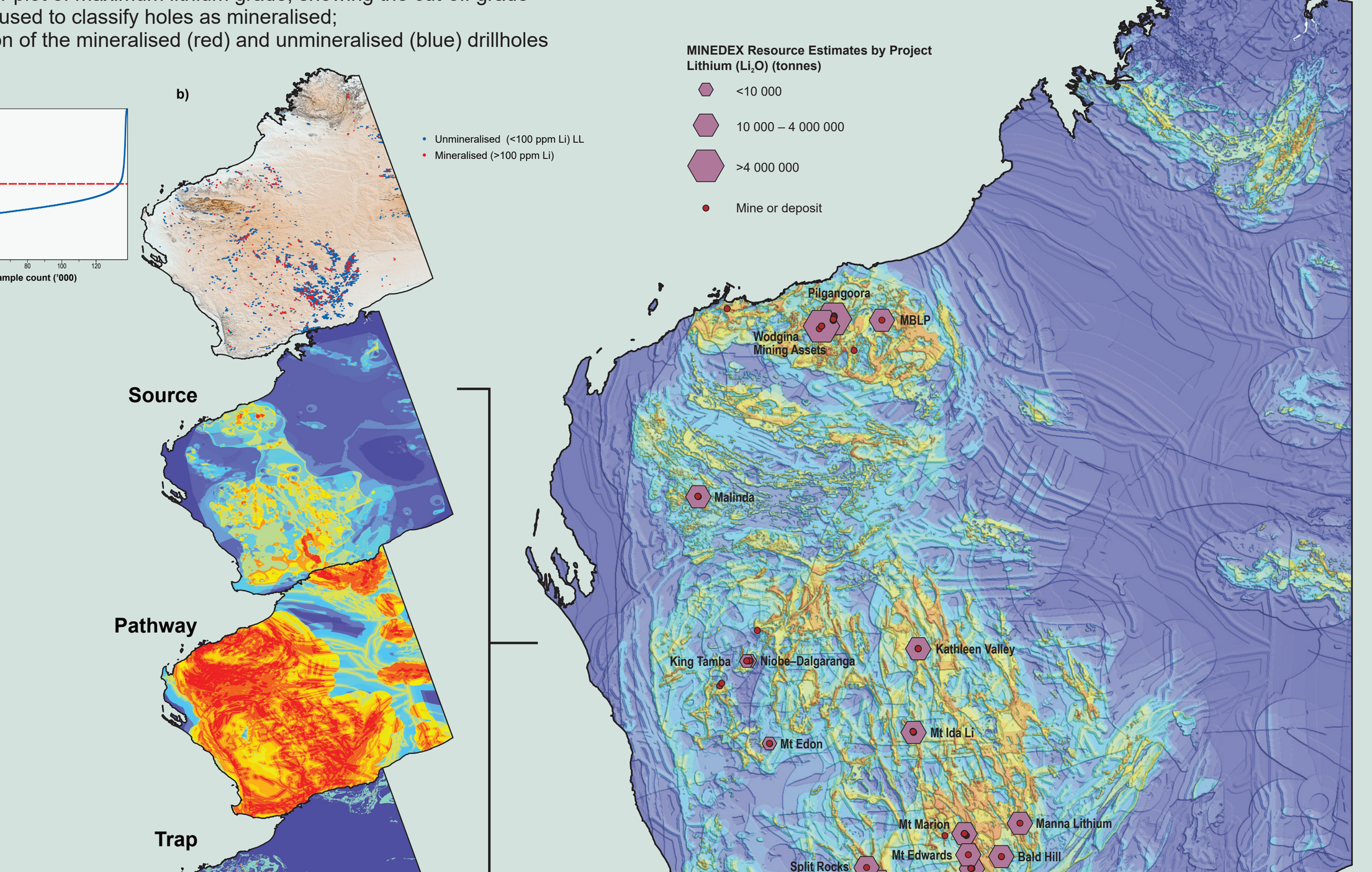

Predictor maps were combined to form a summary map for each major component of the mineral system, and these were then combined to produce the final image. Higher relief and red–orange colours depict higher prospectivity values and lower relief and blue colour depict lower prospectivity values

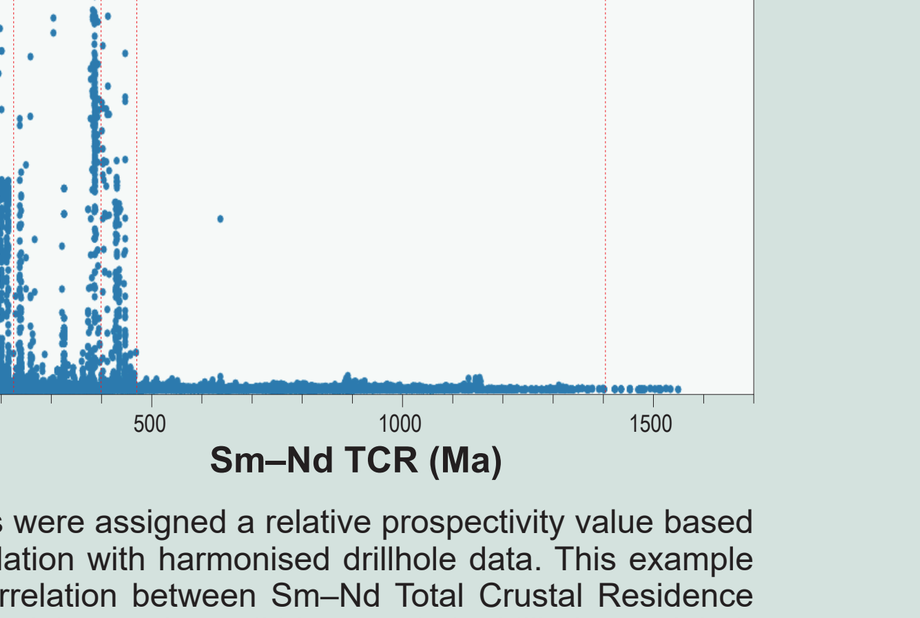

Input datasets were assigned a relative prospectivity value based on their correlation with harmonised drillhole data. This example shows the correlation between Sm–Nd Total Crustal Residence (TCR) times and the maximum lithium grade in drillholes and their relative prospectivity ratings

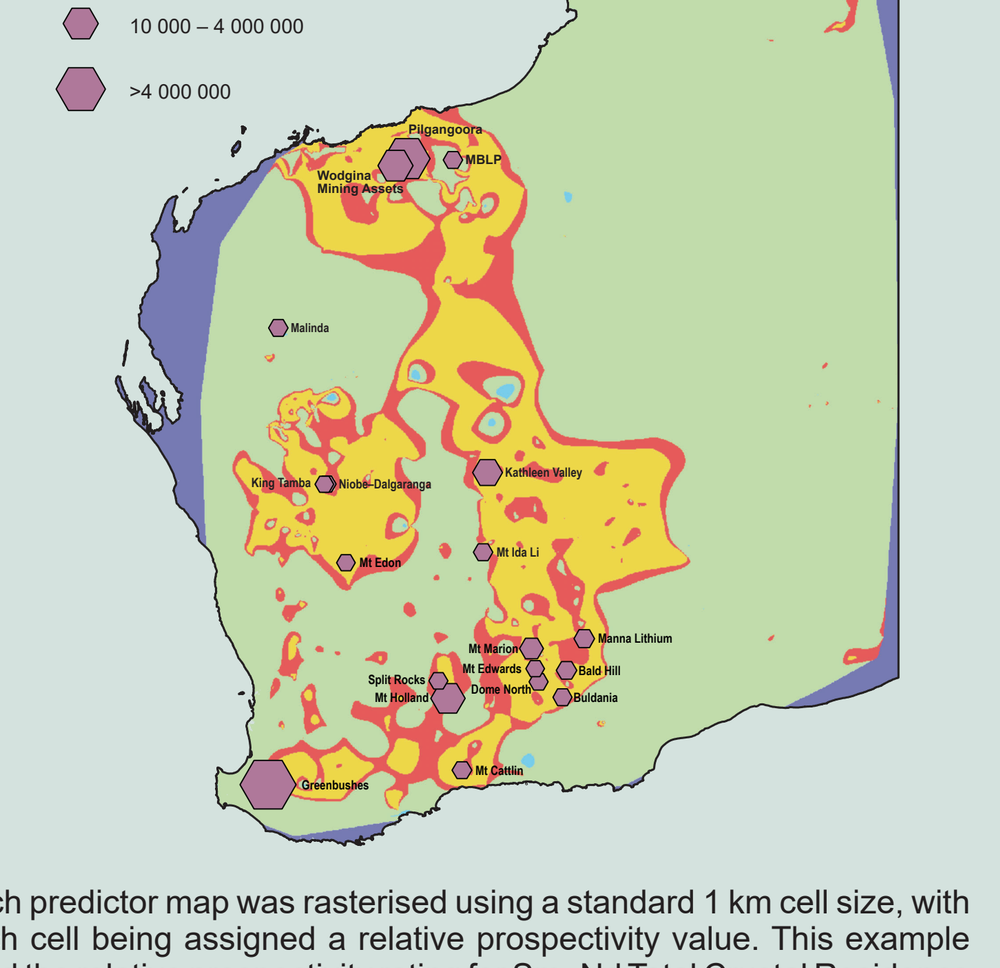

Each predictor map was rasterised using a standard 1 km cell size, with each cell being assigned a relative prospectivity value. This example used the relative prospectivity rating for Sm–Nd Total Crustal Residence times. Red represents the highest rating, orange a medium rating, with green representing the lowest. Blue denotes insufficient data

The Mineral Systems Atlas (MSA) seeks to help anyone who wants to find exploration-relevant spatial data and information presented in a logical mineral systems-based framework. Each system is accompanied by an online MSA Guide and GSWA Record. The online guide presents information on each spatial layer, the primary data from where it was derived, and any filters or query models used. The Li prospectivity map, intermediate predictor maps and input datasets will be published on the MSA and the Data and Software Centre as part of the Rare-element pegmatite system along with an explanatory note Record, allowing the end-user to recreate the map or combine this approach with their own datasets.

Mineral Sytems Atlas

Scan to go to latest release

For more information, contact:
Nathan Bowman (nathan.bowman@demirs.wa.gov.au)

Yilgarn Craton

Radiogenic heat production provides a thermal threshold for cratonisation of the Yilgarn Craton

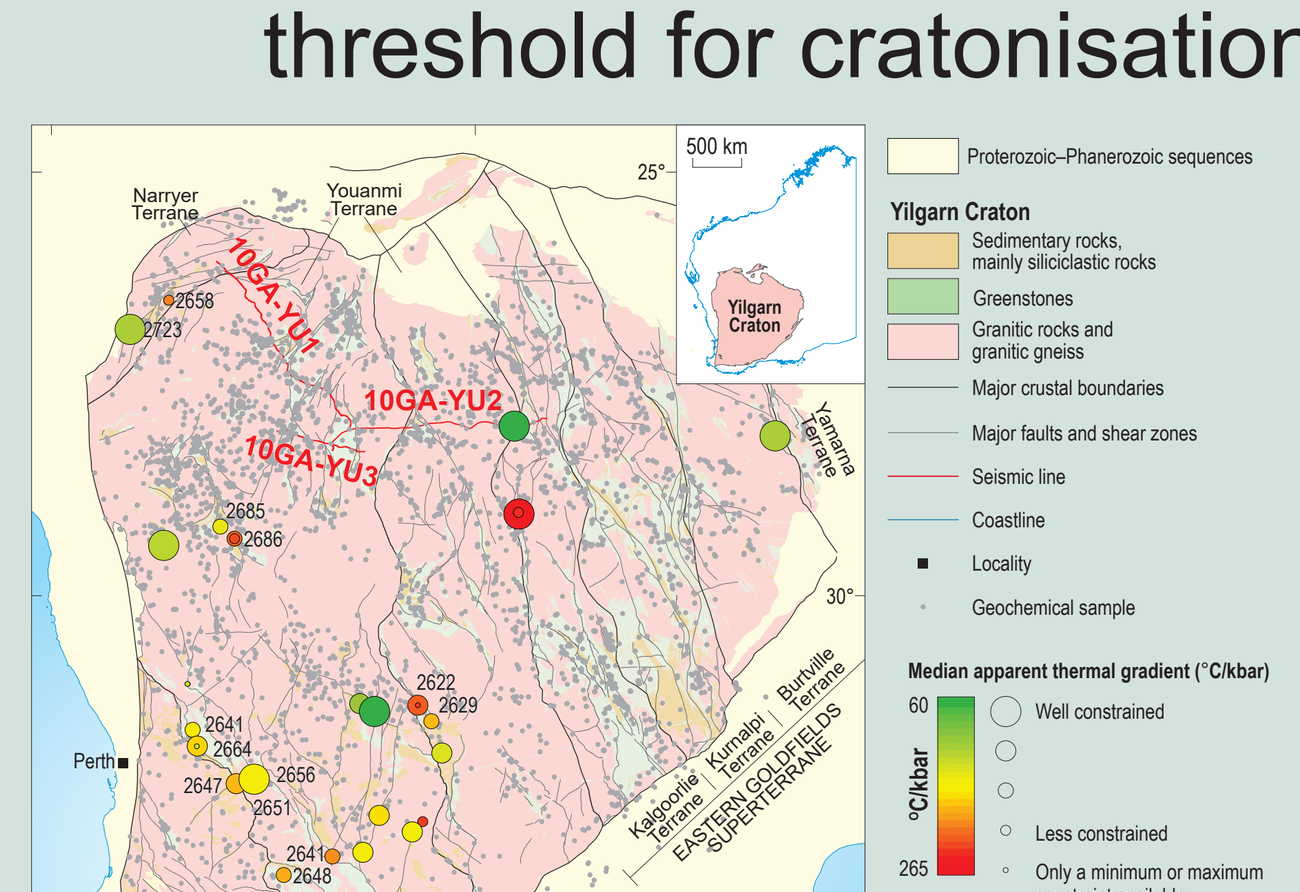

Figure 1. Simplified map of the Yilgarn Craton, showing geochemistry sample locations (n = 5545), Archean metamorphic data (n = 30) plotted as median peak apparent thermal gradient (with peak metamorphic age in Ma), and the location of published (intepreted) seismic lines

The magnitude of radiogenic heat production in the Yilgarn Craton has been underestimated in previous studies, resulting in an underappreciation of its role in crustal evolution and mineralisation (Au ± Ni) processes. It may also play a critical role in promoting the melting of Li-bearing source regions.

A striking feature of the Yilgarn Craton (Fig. 1) at the current erosional level is an abundance of high-K (low-Ca) granites with radiogenic heat production elevated far above global crustal averages (Fig. 2). Extrapolated back in time, the total thickness and contribution to crustal heat production and heat flow from these granites was greater, implying that the deeper crustal sources must also have been elevated in radiogenic heat production.

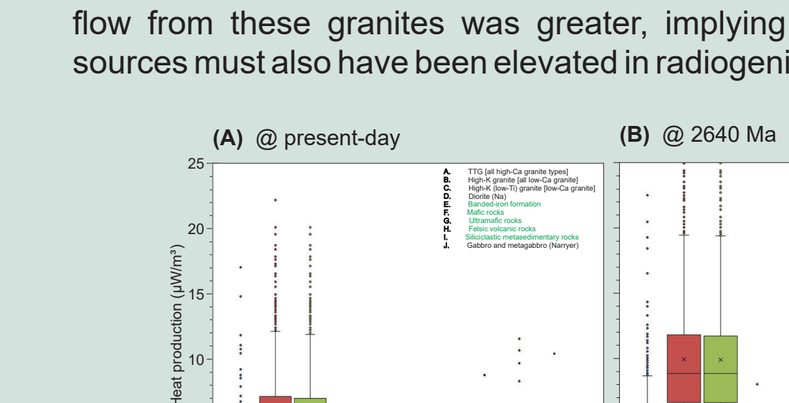

Figure 2. Box and whisker plots of calculated heat production for the key lithological groups considered in this work:
(A) Present-day
(B) 2640 Ma
(1) Grey line is average granite (= 2.5 μW/m³; Haenel et al., 1988)
(2) Red line is mean felsic value for the Yilgarn Craton (= 1.88 μW/m³; Hawkesworth and Jaupart, 2021).
Note some extreme outliers plot beyond the range shown

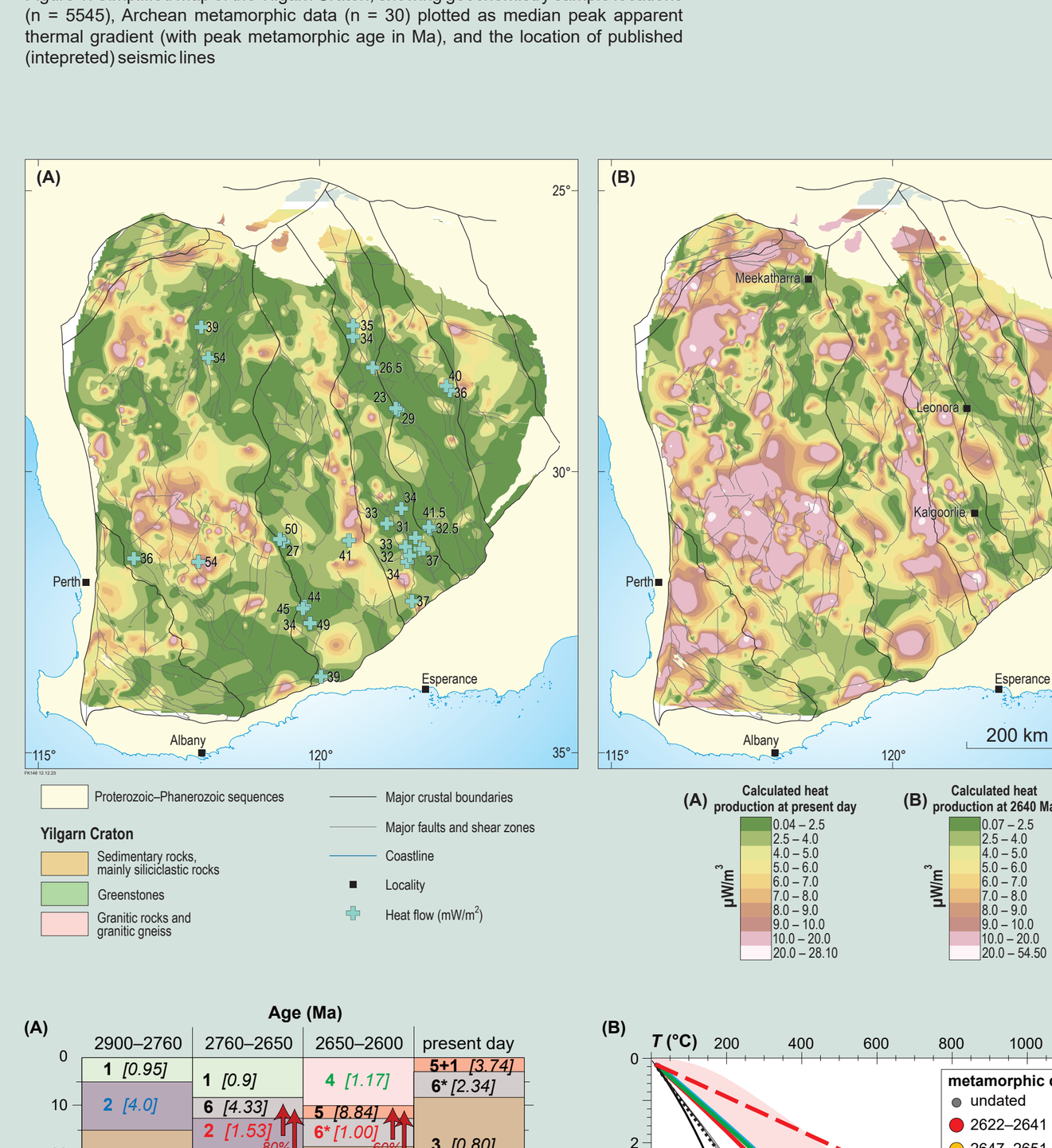

A heat production map (Fig. 3A) shows that vast tracts of the exposed surface have heat production that is significantly higher than global average granite (grey line on Fig. 2A). High-heat production at the surface coupled with low- to moderate surface heat flow (Fig. 3A) implies that modern day heat production at depth must be lower, consistent with extraction of heat-producing elements (K, Th, U) from deeper sources to produce these upper crustal radiogenic granites. The median heat production at 2640 Ma for the felsic groups ranges from 3.5 to 8.8 μW/m³ (Fig. 2B), and the heat production map for 2640 Ma (Fig. 3B) shows that the lithologies at the exposed surface would have had considerable heat production in the past.

Figure 3. Heat production maps of the Yilgarn Craton, based on whole-rock geochemistry of all least-altered samples shown in Figure 1:
(A) Present-day, with surface heat flow
(B) Heat production calculated at 2640 Ma. Maps generated with natural neighbor interpolation using natural breaks in data values
All colours except the darkest green represent heat production values higher than typical crustal values

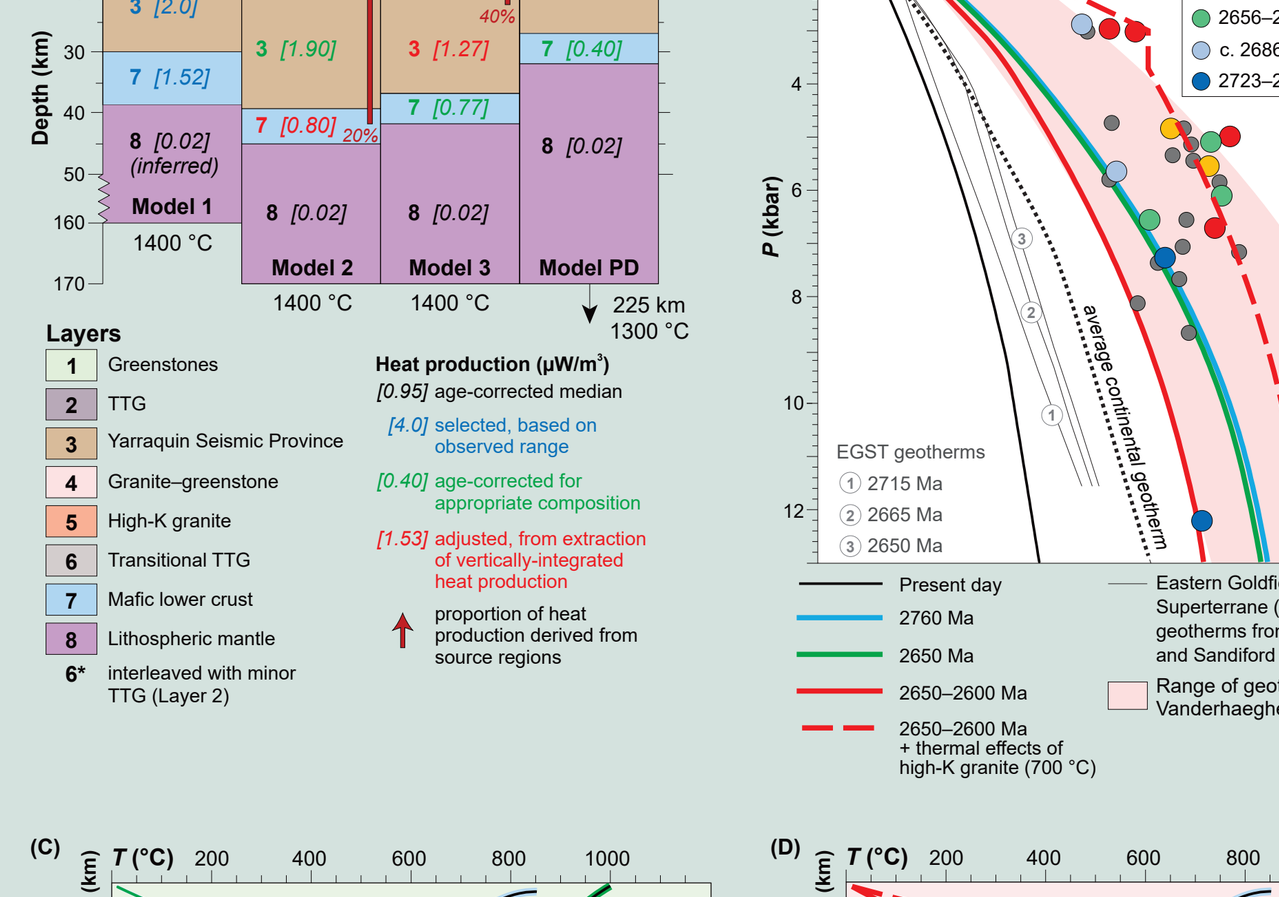

We conducted 1D thermal models underpinned by geological and geochemical constraints. The models attempt to reconstruct a simple but realistic crustal evolution based on the existing stratigraphic and magmatic framework (Fig. 4A).

The modelled thermal gradients at 2760–2650 Ma (blue and green lines; Fig. 4B) capture many of the older metamorphic data, indicating elevated thermal conditions in the crust for 100s Ma.

The younger metamorphic record is best explained by (significant) advective heat (dashed red line, Fig. 4B). That is, the late 'bloom', high-K granites caused an advective thermal regime superimposed on that caused by radiogenic heating alone, resulting in regional contact metamorphism.

Figure 4. Results of the thermal modelling:
(A) Model setup, with calculated heat production values shown in brackets
(B) Calculated thermal gradients and metamorphic data (plotted as median peak P, T); assuming a crustal density of 2.8 g/cm³

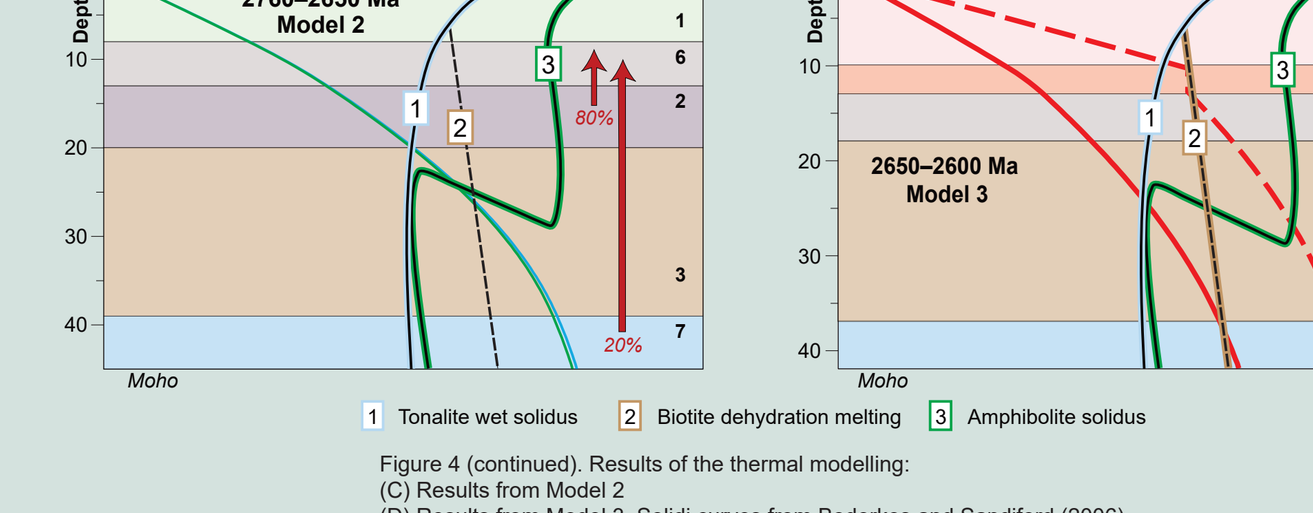

Figure 4 (continued). Results of the thermal modelling:
(C) Results from Model 2
(D) Results from Model 3. Solidi curves from Bodorkos and Sandiford (2006)

The predicted thermal gradients intersect the tonalite wet solidus at about 20 km depth, and both dehydration curves at 25 km (Fig. 4C), implying that for a protracted period the mid to deep crust that was near to, at or above conditions for partial melting, and primed for melting by an internal driver.

Over time, advective movement of progressively more radiogenic heat production to the shallower crust results in two complementary outcomes:

- refractory crust at deeper levels
- long-term cooling

The widespread granite 'bloom' at 2650–2600 Ma records the final time that the crust was fertile enough to melt in large volumes, as well as the thermal gradient being hot enough to intersect the solidus (Fig. 4D).

For more information, contact:
Fawna Korhonen (fawna.korhonen@demirs.wa.gov.au)

References cited:
Bodorkos, S and Sandiford, M 2006, Thermal and mechanical controls on the evolution of Archean crustal deformation: examples from Western Australia, *in* Archean Geodynamics and Environments *edited by* K Benn, J-C Mareschal and KC Condie: American Geophysical Union, Geophysical Monograph Series 164, p. 131–147, doi:10.1029/164GM10.

Vanderhaeghe, O, Guergouz, C, Fabre, C, Duchêne, S and Baratoux, D 2019, Secular cooling and crystallization of partially molten Archaean continental crust over 1 Ga: Comptes Rendus Geoscience, v. 351, no. 8, p. 562–573.

Fortescue Group

Geochemical barcoding

The 2780–2630 Ma Fortescue Basin of the Pilbara provides an opportunity to look at a nearly pristine and continuous Archean volcanic succession, equivalent in age to the greenstone belts of the Eastern Goldfields. This project uses high-quality whole rock major and trace element data from a number of drillholes and detailed outcrop traverses through the igneous rocks of the Fortescue Group, to provide a geochemical barcode for the succession. The geochemical data aids the correlation of the stratigraphy across the whole Fortescue Basin, previously established in several smaller mapping projects. The distribution and petrogenetic interpretations of the data help to uncover the ancient topography to the volcanic eruptions and identify major rift zones and fissures.

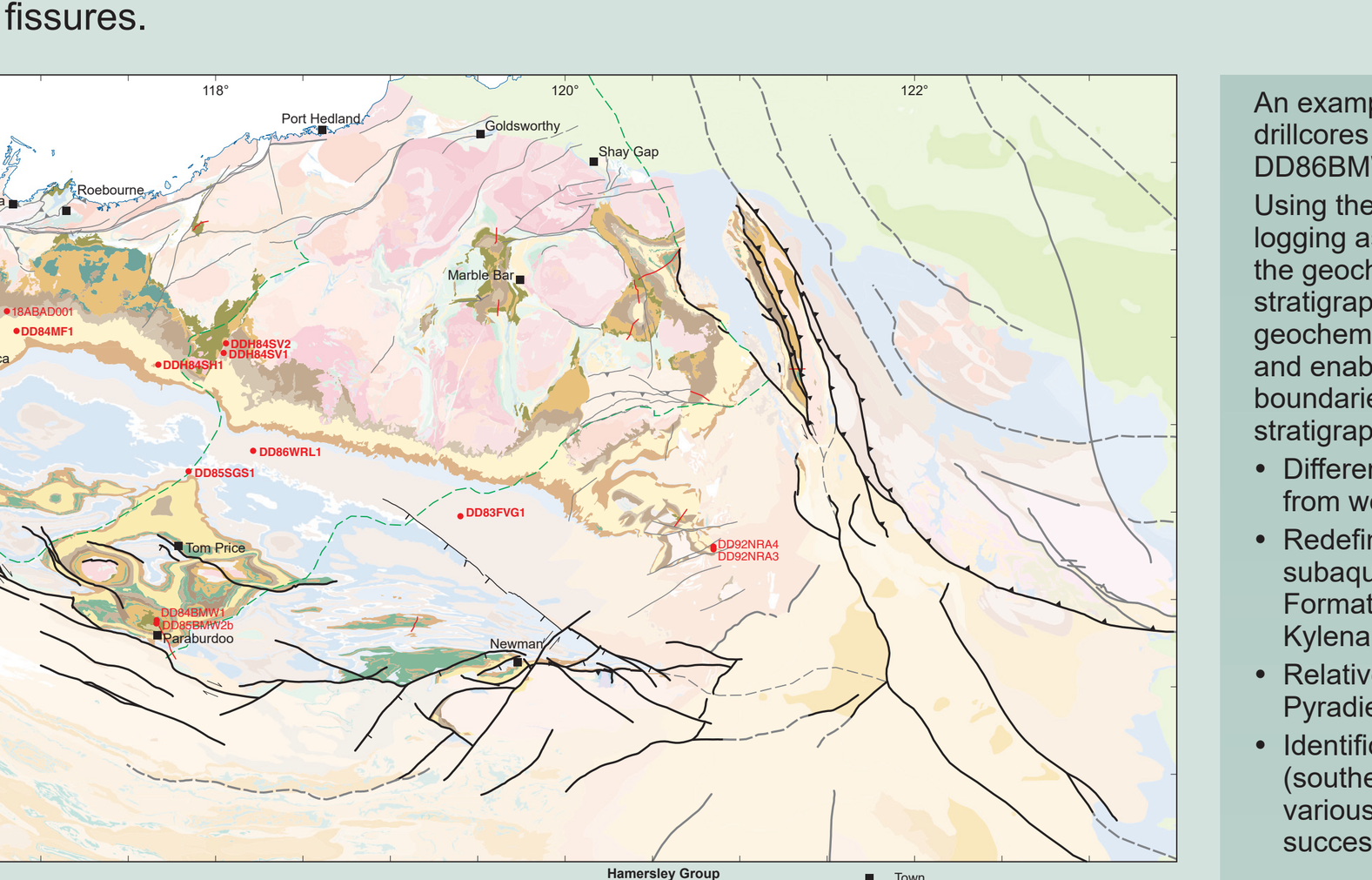

An example of correlated stratigraphic logs of drillcores from DD84MF1, DD86WRL1, DD86BMW1 and DD86BMW2b.

Using the previous mapping and drillcore logging as a basis for the broad stratigraphy, the geochemical sampling throughout the stratigraphy has identified several geochemical groups within each formation and enabled us to refine the formation boundaries. The main modifications to the stratigraphy include:

- Differences between Mount Roe Basalt from west to east
- Redefining the boundary between the subaqueous basalts of the Boongal Formation and subaerial basalts of the Kylena Formation
- Relative timing of the Tumbiana and Pyradie Formations
- Identification of fissures and main rift zones (southern and eastern Pilbara margins) at various times during the deposition of the succession

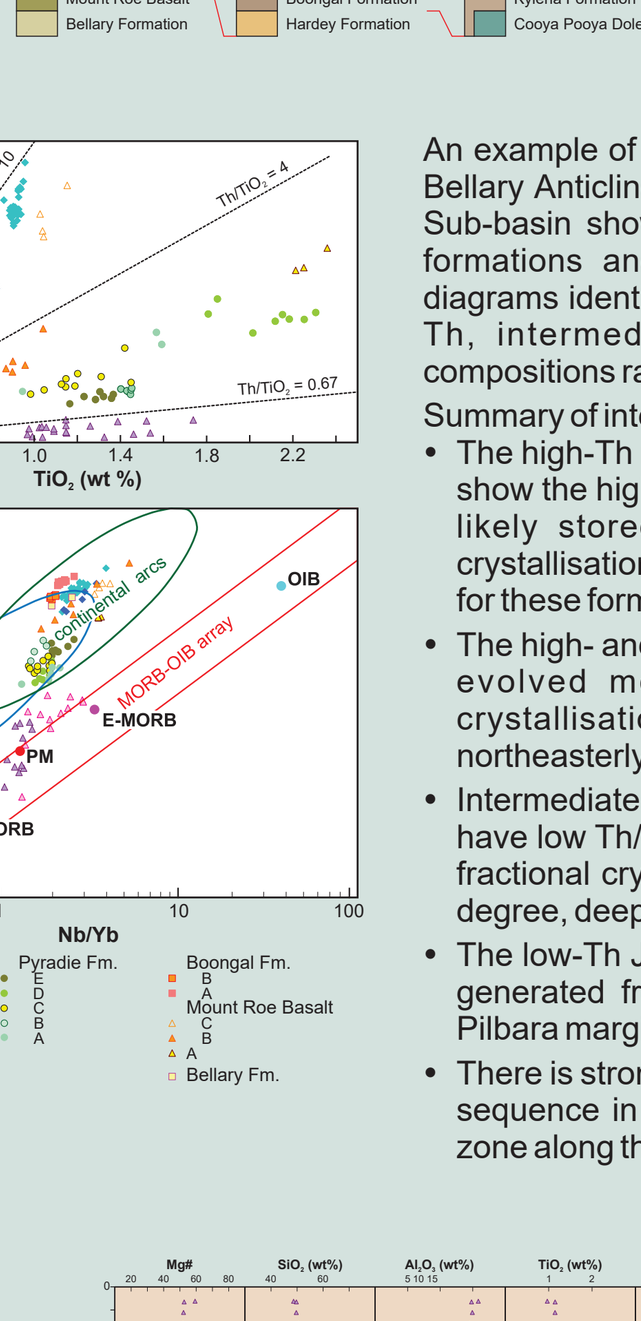

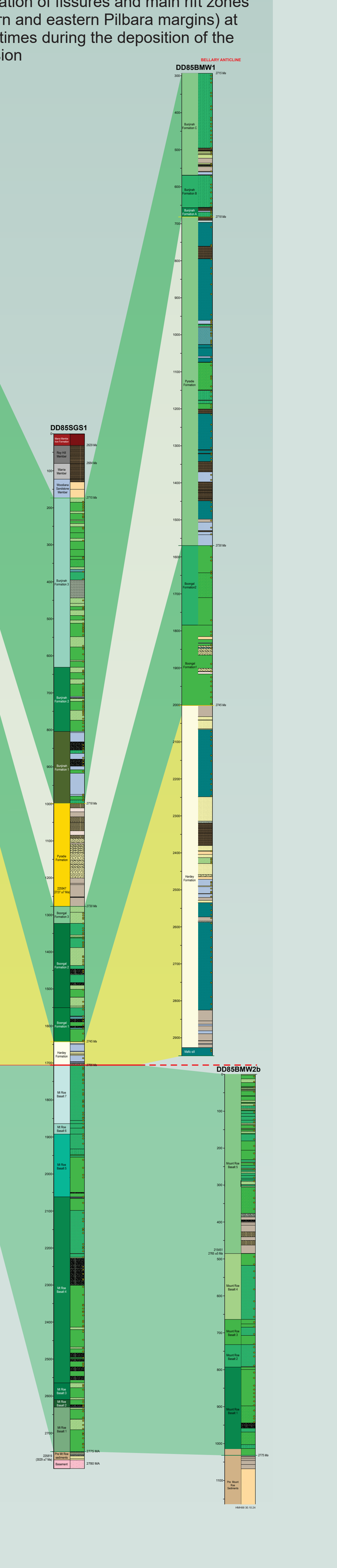

An example of data from a detailed geochemical traverse in the Bellary Anticline near the southern margin of the South Pilbara Sub-basin shows significant geochemical variation both within formations and up the stratigraphy. Geochemical variation diagrams identify compositionally unique units that fall into high-Th, intermediate-Th and low-Th groups (a) and have compositions ranging from the MORB to Continental Arc fields (b).

Summary of interpretations:

- The high-Th magmas of the Boongal and Bunjinah Formations show the highest degree of crustal assimilation and were most likely stored in the crust prior to eruption. Fractional crystallisation is a secondary control with more limited influence for these formations, suggesting their rapid emplacement.
- The high- and intermediate-Th groups of the Mount Roe Basalt evolved mostly through assimilation and fractional crystallisation processes and were fed through north-northeasterly-trending Black Range dykes.
- Intermediate-Th groups such as those of the Pyradie Formation have low Th/Yb, suggesting minimal crustal contamination but fractional crystallisation is a stronger control. They are higher degree, deeper melts, potentially of plume origin.
- The low-Th Jeerinah Formation has MORB-like geochemistry, generated from depleted upper mantle, along the southern Pilbara margin and consistent with passive margin setting.
- There is strong evidence to suggest that much of the Fortescue sequence in the South Pilbara Sub-basin was fed from a rift zone along the southern margin of the Pilbara.

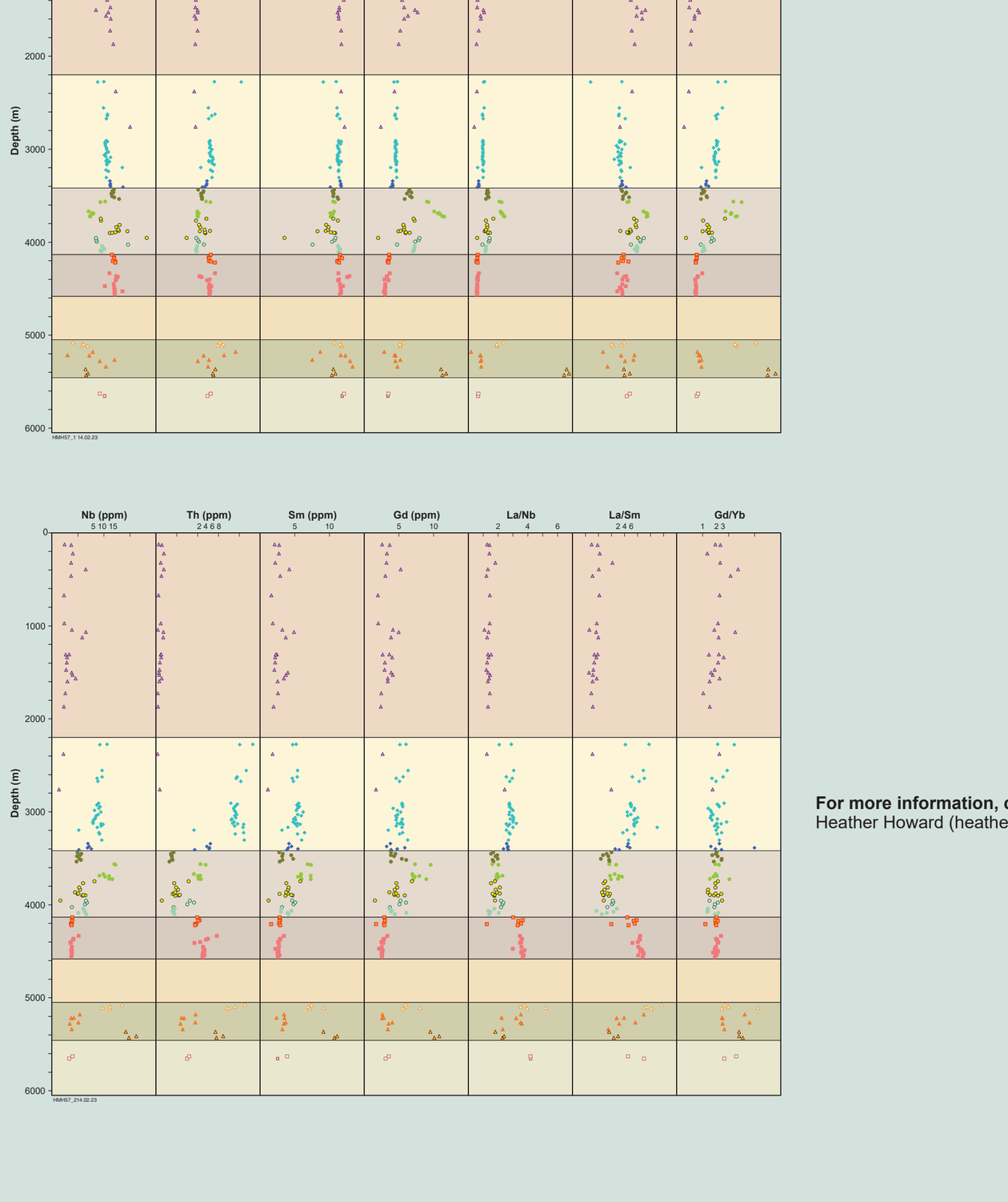

For more information, contact:
Heather Howard (heather.howard@demirs.wa.gov.au)

Officer Basin

Sediment-hosted copper shows

As nations embrace renewable energy transitions and the expansion of digital technologies, the demand for copper is poised for significant growth. Covering roughly 12% of Western Australia (WA), the Officer Basin has the potential to contain economic sediment-hosted copper (SedCu) deposits but remains mostly underexplored. Initial Geological Survey of Western Australia (GSWA) investigations into Officer Basin legacy data and material have yielded significant shows of subeconomic copper mineralisation or enrichment with SedCu signatures.

- The intracratonic Officer Basin is predominantly Neoproterozoic, overlying older Mesoproterozoic to Archean sedimentary, igneous and metamorphic rocks.
- An initial review of the basin's stratigraphy and characteristics showed a conceptual fit for the SedCu mineral system.
- A review of legacy data and reports, including from petroleum exploration, found several occurrences of SedCu indicators.
- GSWA core library drill core with SedCu indicators or potential trap lithologies were selectively sampled, with results further supporting the hypothesis.
- These initial investigations focused on the lesser explored central and eastern areas of the WA Officer Basin.
- More work to follow, including further sampling of legacy material and basin analysis.

The standard SedCu mineral system model after Hitzman et al. (2005) ideally requires an intracratonic basin with: (a) a copper source in the form of basal oxidised siliciclastic, volcanic or basement rock units; (b) a carbonate–evaporite hydrologic seal to help supply and constrain Cu-scavenging brines to the basal oxidised units; (c) a trigger that initiates Cu-enriched brine flow up the stratigraphy, in conjunction with; (d) fluid pathways such as faults, unconformities, stratigraphic pinchouts, or salt diapirs, transporting and focussing the Cu-enriched brines to; (e) a reductant in the form of reduced lithologies (e.g. carbonaceous siltstones — a reduced facies deposit style), mobile hydrocarbons (e.g. Sour Gas - H_2S - a sandstone/Revett deposit style), or organic matter (a redbed deposit style).

These mineral system components are present within the Officer Basin as (a) Basal sandstone units, Archean (Yilgarn) and Mesoproterozoic basement units; (b) Browne Formation salt and carbonate units; (c) and (d) Multiple regional orogenies, mafic volcanism, salt tectonics, faulting and basin compaction; (e) reducing lithologies within Tonian formations, hydrocarbons or organic matter throughout the stratigraphic sequence (at time of mineralisation).

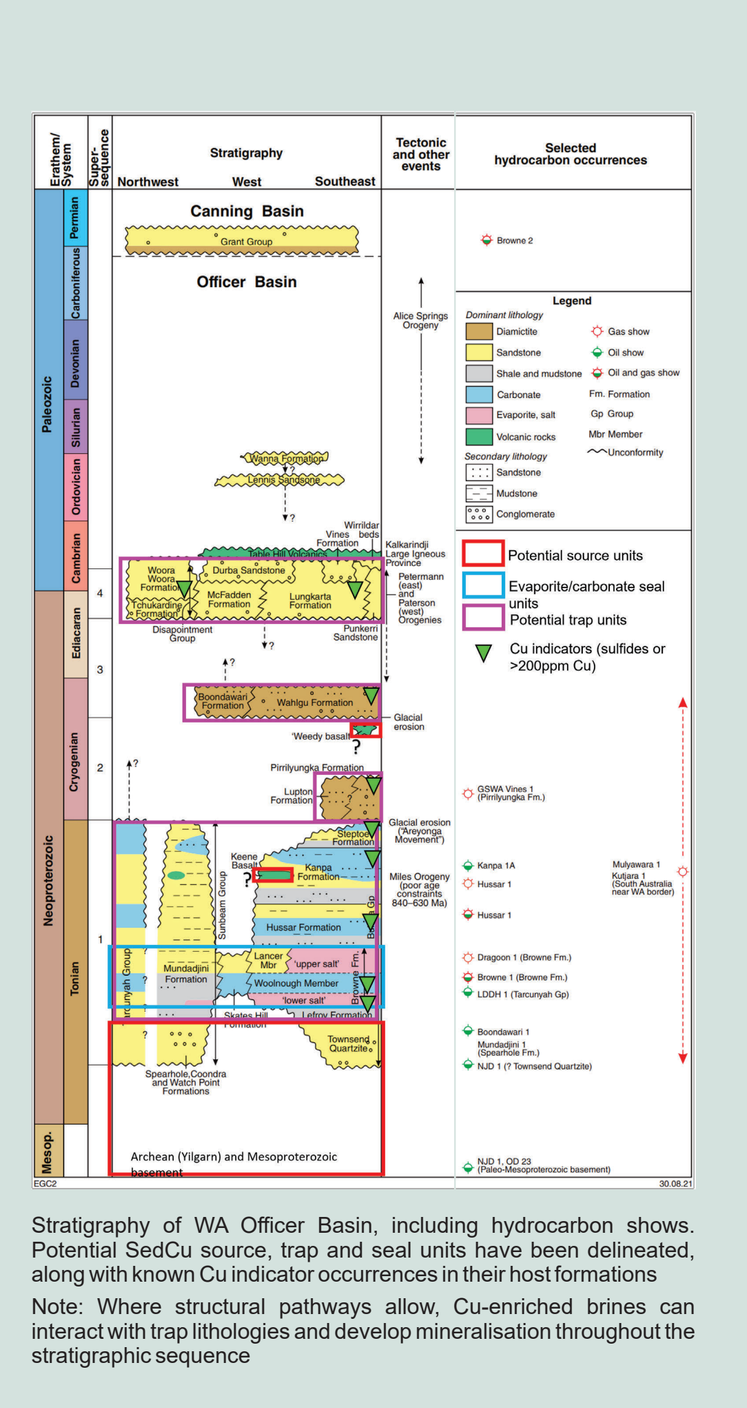

Stratigraphy of WA Officer Basin, including hydrocarbon shows. Potential SedCu source, trap and seal units have been delineated, along with known Cu indicator occurrences in their host formations

Note: Where structural pathways allow, Cu-enriched brines can interact with trap lithologies and develop mineralisation throughout the stratigraphic sequence

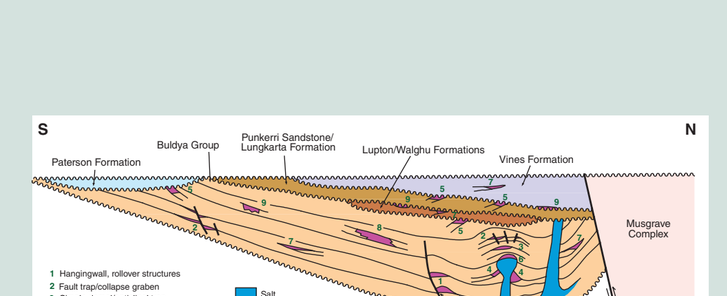

Schematic of possible hydrocarbon traps in the eastern WA Officer Basin, which includes GSWA Vines 1, from D'Ercole et. al. (2005). These structures could also act as pathways or traps for Cu-enriched brines, with reducing lithologies or hydrocarbons/organic matter acting as reductants. The salt rupture zone of the Officer Basin presents opportunities for basal Cu-enriched brines to traverse much of the stratigraphic sequence

Formation	Age	Cu sulfide observation	Cu assay 90–200 ppm	Cu assay 200–1000 ppm	Cu assay >1000 ppm	Host lithology	Drillholes/wells (more significant first)
Woora Woora	Ediacaran–Cambrian					Sandstone, siltstone, (incl. stromatolitic)	BH01 BH02
Lungkarta	Ediacaran–Cambrian	●				Sandstone	Hussar 1
Wahlgu	Cryogenian	●				Diamictite/sandstone, Calcareous siltstone	GSWA Vines 1 Hussar 1
Pirrilyungka	Cryogenian	●				Siltstone/mudstone (dolomitic)	GSWA Vines 1
Steptoe	Tonian	●				Dolomite (incl. vuggy), very fine grained sandstone/siltstone	GSWA Empress 1A
Kanpa	Tonian					Siltstone, shale	GSWA Lancer 1 Lungkarta-1/ST1
Hussar	Tonian	●				Carbonate siltstone, calcareous sandstone	Hussar 1
Woolnough Member	Tonian	●				Dolomitic conglomerate	OB002
Lower Browne	Tonian	●				Sandstone, dolomite (incl. stromatolitic), anhydrite+carb veins, anhydrite-mudstone, mudstone	OB002, Dragoon 1 Yowalga3

Officer Basin sedimentary formations, their observed copper indicators and host lithologies. Cu sulfides range from trace chalcopyrite to sub-economic bornite–chalcocite–chalcopyrite mineralisation

Note: Despite none of the above drillholes or wells specifically targeting SedCu deposits — and with only BH01 and BH02 focusing on metalliferous commodities — they still revealed several occurrences of trace sulfides to subeconomic mineralisation, highlighting the Officer Basin's potential

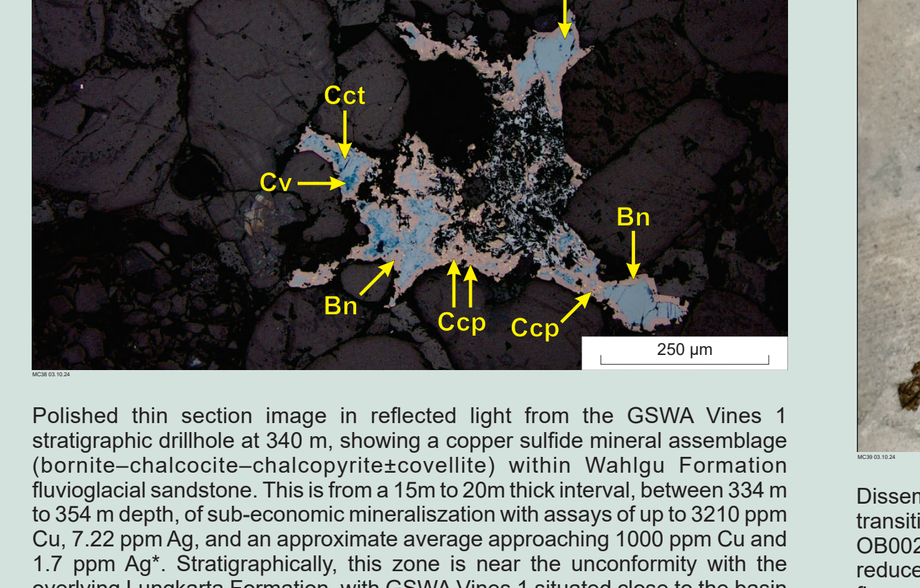

Polished thin section image in reflected light from the GSWA Vines 1 stratigraphic drillhole at 340 m, showing a copper sulfide mineral assemblage (bornite–chalcocite–chalcopyrite±covellite) within Wahlgu Formation fluvioglacial sandstone. This is from a 15m to 20m thick interval, between 334 m to 354 m depth, of sub-economic mineralization with assays of up to 3210 ppm Cu, 7.22 ppm Ag, and an approximate average approaching 1000 ppm Cu and 1.7 ppm Ag*. Stratigraphically, this zone is near the unconformity with the overlying Lungkarta Formation, with GSWA Vines 1 situated close to the basin margin with the Musgrave Province. This may represent an unconformity and basin margin stratigraphic pinchout trap, with a chemical reductant in the form of mobile hydrocarbons or organic matter
*estimated from discontinuous sampling

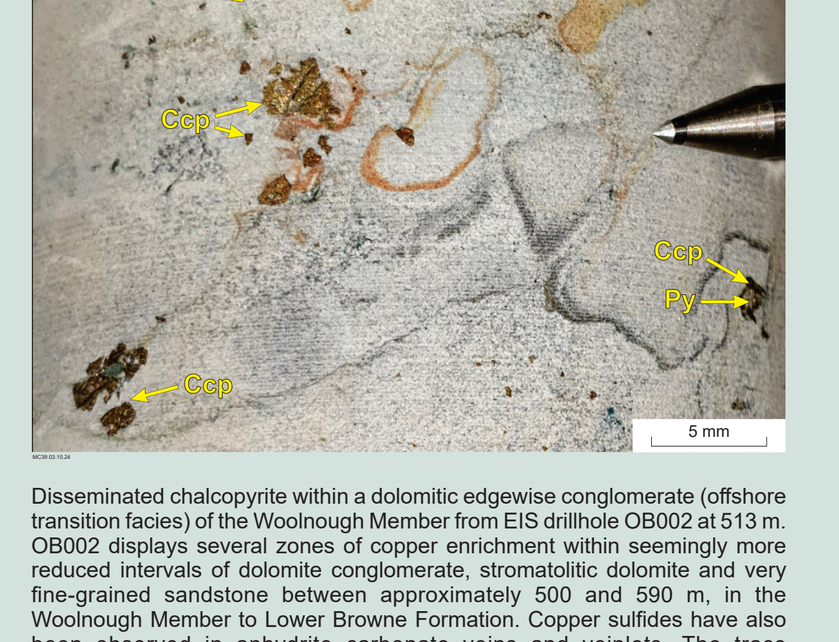

Disseminated chalcopyrite within a dolomitic edgewise conglomerate (offshore transition facies) of the Woolnough Member from EIS drillhole OB002 at 513 m. OB002 displays several zones of copper enrichment within seemingly more reduced intervals of dolomite conglomerate, stromatolitic dolomite and very fine-grained sandstone between approximately 500 and 590 m, in the Woolnough Member to Lower Browne Formation. Copper sulfides have also been observed in anhydrite–carbonate veins and veinlets. The trace mineralisation in this drillhole may represent a more reduced facies style. Of note, the drillhole is located only 4 km southwest from an interpreted major lithospheric structure, and 30 km southwest of the basin's northern margin

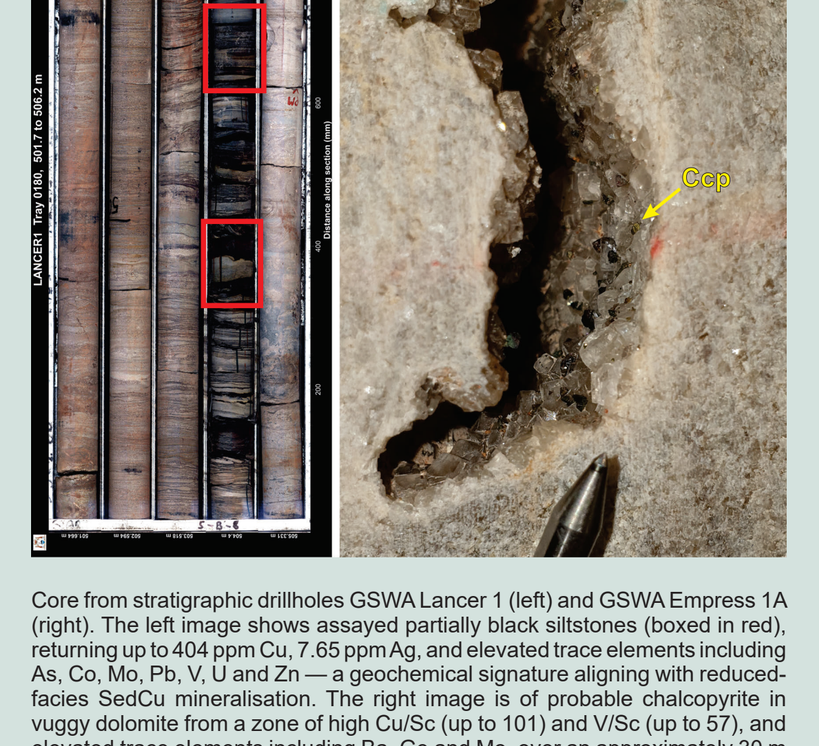

Core from stratigraphic drillholes GSWA Lancer 1 (left) and GSWA Empress 1A (right). The left image shows assayed partially black siltstones (boxed in red), returning up to 404 ppm Cu, 7.65 ppm Ag, and elevated trace elements including As, Co, Mo, Pb, V, U and Zn — a geochemical signature aligning with reduced-facies SedCu mineralisation. The right image is of probable chalcopyrite in vuggy dolomite from a zone of high Cu/Sc (up to 101) and V/Sc (up to 57), and elevated trace elements including Ba, Ge and Mo, over an approximately 30 m thick interval. These two examples are from drillholes over 250 km apart yet show copper enrichment at similar depths (approximately 500 m) and at a similar stratigraphic position — near the unconformity with the overlying Wahlgu Formation

For more information, contact:
Matt Clarke (matt.clarke@demirs.wa.gov.au)

Minerals geoscience

GSWA has identified several new occurrences of trace to subeconomic copper mineralisation in the central and eastern WA Officer Basin. These, along with legacy data and recent modelling by Geoscience Australia (Cloutier et al., 2023), support the potential for SedCu deposits in the Officer Basin. Ongoing work, along with other GSWA initiatives, such as WA Array, could help narrow the search space for SedCu deposits in the Officer Basin.

www.demirs.wa.gov.au